American Mineralogist, Volume 90, pages 1563–1570, 2005

Light-induced degradation dynamics in realgar: in situ structural investigation using single-crystal X-ray diffraction study and X-ray photoelectron spectroscopy

ATSUSHI KYONO,[1,*] MITSUYOSHI KIMATA,[1] AND TAMAO HATTA[2]

[1]Division of Earth Evolution Sciences, Graduate School of Life and Environmental Sciences, University of Tsukuba, Tennodai 1-1-1, Tsukuba, Ibaraki 305-8572, Japan

[2]Japan International Research Center for Agricultural Sciences, Ohwashi 1-1, Tsukuba, Ibaraki 305-8686, Japan

ABSTRACT

Light-induced degradation in realgar (arsenic sulfide) has been studied by means of four-circle single-crystal X-ray diffraction and X-ray photoelectron spectroscopy. Because of the alteration of realgar exposed to light, the *a* lattice parameter and *c* sinβ value increase linearly from 9.327 to 9.385 Å and from 6.320 to 6.364 Å, respectively. In contrast, the *b* lattice parameter remains substantially constant. Anisotropic variations of the lattice parameters engender a continuous increase of the unit-cell volume from 799.5 to 810.4 Å^3. Nevertheless, no correlation exists between the continuous increase of the unit-cell volume and the bond distance variations in As_4S_4 molecules because the As_4S_4 molecule in the unit cell expands very little during light exposure. The most pronounced change was in the distance between centroids in As_4S_4 cages. The spread of As_4S_4 intermolecular distances increases continuously from 5.642 to 5.665 Å, which directly affects the unit-cell volume expansion of realgar. In addition, the O1s peak increases rapidly after light exposure. The result substantiates the following reaction proposed by Bindi et al. (2003): $5As_4S_4 + 3O_2 \rightarrow 4As_4S_5 + 2As_2O_3$. That is, realgar is transformed into pararealgar if oxygen exists and produces the As_4S_5 molecule. The additional S atom contributes to anisotropic expansion for the **a** and **c** axes because the direction of the additional S atom points toward [4$\bar{1}$4] in the unit cell. Furthermore, an S atom in the As_4S_5 molecule is released from one of the equivalent As-S-As linkages in As_4S_5 which becomes the As_4S_4 molecular of pararealgar. After the As_4S_5 molecule is divided into an S atom (radical) and the As_4S_4 (pararealgar type) molecule, the free S atom is re-attached to another As_4S_4 (realgar type) molecule, and reproduces an As_4S_5 molecule. The reproduced As_4S_5 molecule is again divided into an S atom (radical) and an As_4S_4 (pararealgar type) molecule. This cycle whereby realgar is indirectly transformed into pararealgar via the As_4S_5 molecule is promoted by light and repeated during light exposure.

INTRODUCTION

Many studies have addressed crystal structures, phase transitions, and stability fields of the As_4S_4 polymorphs: realgar (α-As_4S_4) (Ito et al. 1952; Pen'kov and Safin 1972; Forneris 1969; Mullen and Nowacki 1972; Bues et al. 1983; Bryndzia and Kleppa 1988), pararealgar (Roberts et al. 1980; Douglass et al. 1992; Bonazzi et al. 1995), χ phase (Douglass et al. 1992; Bonazzi et al. 1996), and the high-temperature phase (β-As_4S_4) (Clark 1970; Street and Munir 1970; Porter and Sheldrick 1972; Roland 1972; Yu and Zoltai 1972; Burns and Percival 2001; Bonazzi et al. 2003). The exposure of realgar to light engenders alteration to friable yellow-orange thin films or micro-nodules on the surface and fissures at some critical thickness, causing degradation (Roberts et al. 1980; Douglass et al. 1992). The yellow-orange products covering the realgar consist of pararealgar, which transforms with light at wavelengths between about 500 and 670 nm (Douglass et al. 1992). Such alteration always proceeds from realgar via χ phase to pararealgar. Douglass et al. (1992) proposed that light breaks As-As bonds, which are weaker than As-S bonds. Thereby, the covalently bonded cage molecules form a new crystal structure in which free As is intercalated. Bonazzi et al. (1996) showed that formation of the χ phase is preceded by a strong anisotropic increase of the unit-cell volume of realgar: *a* and *c* sinβ increase linearly with increasing exposure times, whereas *b* remains substantially unchanged. The authors documented that the unit-cell volume is between 798–800 Å^3 before light treatment; it reaches up to 810 Å^3 after 300 min of exposure. Subsequently, Bonazzi et al. (1996) concluded that the χ phase can be considered as an expanded, less-ordered β phase. Bindi et al. (2003) studied the crystal structure of uzonite (As_4S_5) and the variability if its unit-cell parameters with light exposure. Results obtained in that study indicate that the As_4S_5 molecules remain unchanged, in contrast to the As_4S_4 molecules. Non-stoichiometric As_8S_{9-x} crystals, which consists of a disordered mixture of As_4S_4 and As_4S_5 molecules, also point toward a light-induced increase of the unit-cell volume (Bonazzi et al. 2003). They reported that the increase in unit-cell volume may be caused by increasing of sulfur in the structure because the unit-cell volume of arsenic sulfides (see Bonazzi et al. 2003, their Fig. 4) increases linearly with an increase in the percentage of As_4S_5 molecules. Very recently Ballirano and Maras (2004) reported an increase in the unit-cell volume of realgar caused by the partial replacement of As_4S_4 cages by As_4S_5 cages. Bonazzi et al. (2003) suggested that an increase in the percentage of As_4S_5 molecules in the structure

* E-mail: kyono@arsia.geo.tsukuba.ac.jp

0003-004X/05/0010–1563$05.00/DOI: 10.2138/am.2005.1785

could occur if the following reaction takes place: $5As_4S_4 + 3O_2 \rightarrow 4As_4S_5 + 2As_2O_3$. Indeed, the formation of arsenolite in the light-induced process of alteration of realgar to pararealgar has been reported (Ballirano and Maras 2002). Furthermore, recent X-ray photoelectron spectroscopy investigations of core-level binding energies of As_4S_4 polymorphs have proven that there is little difference (less than 0.1 eV) in the binding energy shifts of realgar and pararealgar (Bullen et al. 2003). A small concentration of arsenic oxide species, probably As_2O_3, was also found on the crystal surfaces (Bullen et al. 2003).

The present study addresses structural dynamics during light-induced degradation in realgar using in situ single crystal X-ray diffraction methods. We studied chemical alterations using in situ X-ray photoelectron spectroscopy.

Experimental methods

The sample of realgar used in the present experiment is from the Getchell mine, Nevada. Realgar crystals were hand picked under a binocular microscope, then ground and sieved to a grain size between 150 and 300 µm. Powder X-ray diffraction study indicated only the presence of realgar (α-As_4S_4): no impurities or other As_4S_4 polymorphs were detected.

A quartz-tungsten-halogen lamp (Philips Japan, Ltd.) produced light-induced transformations. Realgar crystals investigated here were exposed to full-spectrum radiation from the lamp. The approximate wavelength was in the range of 350–850 nm. The power density measured with a spectroradiometer (MS-720; Eko Instruments Co., Ltd.) was about 10 mW/cm^2. The electronic apparatus was equipped with an optical fiber bundle to minimize overheating.

Single-crystal X-ray diffraction

The entire X-ray apparatus was completely covered with a blackout curtain to exclude the possibility that the realgar crystal is altered into pararealgar by other light sources during measurement. A suitable single crystal of prismatic shape (0.20 × 0.20 × 0.10 mm in size) was selected for structural study and mounted on an Enraf-Nonius CAD4 four-circle X-ray diffractometer (XRD) using graphite-monochromatized Mo*K*α radiation (λ = 0.7103 Å) at room temperature: 20 ± 1 ºC. The front of the optical fiber was placed at a distance of about 15 mm from the crystal. Structural measurements were performed after light exposure for each 6 h step. The unit-cell parameters were determined by least-squares refinement of the setting angles of the same 25 reflections ($11 < \theta < 14^o$) (Table 1). Intensity data were measured in the 2–30º θ range using ω-2θ scan mode. The data were corrected for Lorentz and polarization factors with the SDP program system (Enraf Nonius 1983). An empirical absorption correction using the ψ-scan technique was applied. The diffraction experiments were continued until loss of crystallinity of the single-crystal. Structural refinements were performed with the SHELXL-97 program (Sheldrick 1997). Several refinement cycles were carried out using first isotropic, then anisotropic thermal displacement parameters. Table 1 summarizes the crystallographic data and details of the refinements. Tables 2 and 3 list atomic coordinates, atomic displacement parameters, intramolecular bond distances and angles.

X-ray photoelectron spectroscopy

The sieved realgar crystals were placed in a glass petri dish 30 mm in diameter. The optical fiber was set toward the samples at a distance of about 15 mm on a 1.3 mm thick glass lid. The sample was then irradiated with the lamp in air through the lid. After light exposure treatment for 6, 12, 18, 24, and 30 h, each sample was immediately mounted on indium foils onto a sample holder made of molybdenum metal. High-resolution X-ray photoelectron spectra (XPS) were collected using an ESCA-300 (Scienta K.K.) instrument with a monochromatized Al*K*α X-ray source (1486.6 eV) and a base pressure of 1.0×10^{-9} torr in the analytical chamber. According to Bullen et al. (2003), no chemical changes were seen after acquiring photoemission spectra with several cumulative X-ray exposures up to several hours. Special care was taken to reduce ambient light exposure by covering the vacuum chamber windows and minimizing ionization gauge use. Survey scans and narrow region scans were collected using 300 and 150 eV pass energies, respectively. The spectrometer work function was adjusted to give a value of 285.0 eV for the C1s peak of adventitious carbon, which is most commonly observed on the surfaces of materials as residual gas in the vacuum. Binding energies measured in each region are summarized in Table 4 and shown later in the paper. Furthermore, to clarify whether or not the concentrations of oxygen were associated with the transformation, we performed the light-alteration experiment in the ESCA-300 instrument. Then, the sample was irradiated with the lamp through the vacuum chamber window under ultrahigh vacuum conditions (1.0×10^{-9} torr).

Table 1. Crystal data and refinement details

Chemical formula		As_4S_4	
Temperature (K)		293	
Formula weight		427.93	
Crystal dimensions (mm)		0.20 × 0.20 × 0.10	
Exposure time (h)	0	6	12
Crystal system	monoclinic	monoclinic	monoclinic
Space group	$P2_1/c$	$P2_1/c$	$P2_1/c$
a (Å)	9.327(2)	9.343(7)	9.360(7)
b (Å)	13.563(1)	13.561(2)	13.573(2)
c (Å)	6.590(2)	6.580(6)	6.590(6)
β (°)	106.46(1)	106.10(3)	105.71(3)
V (Å^3)	799.5(3)	801.0(9)	806(1)
Z	4	4	4
$2\theta_{max}$ (°)	59.92	59.95	59.87
Index ranges	$-13 \le h \le 12$	$-13 \le h \le 12$	$-13 \le h \le 12$
	$0 \le k \le 19$	$0 \le k \le 19$	$0 \le k \le 19$
	$0 \le l \le 9$	$0 \le l \le 9$	$0 \le l \le 9$
D_{calc} (g/cm^3)	3.555	3.548	3.527
Absorption coefficient; Mo*K*α (mm^{-1})	17.52	17.48	17.38
F(000)	784.0	784.0	784.0
Collected reflections	2616	2622	2626
Unique reflections	2327	2333	2336
Observed reflections [$F_o > 4\sigma(F_o)$]	1783	1371	1259
Final *R* [$F_o > 4\sigma(F_o)$]	0.047	0.077	0.081
Largest diffraction peak and hole (e/Å^3)	1.97, –1.01	2.03, –1.56	1.60, –1.19
Exposure time (h)	18	24	
Crystal system	monoclinic	monoclinic	
Space group	$P2_1/c$	$P2_1/c$	
a (Å)	9.380(8)	9.385(5)	
b (Å)	13.569(2)	13.570(1)	
c (Å)	6.593(8)	6.600(5)	
β (°)	105.55(4)	105.36(3)	
V (Å^3)	808(1)	810.4(8)	
Z	4	4	
$2\theta_{max}$ (°)	59.93	60.07	
Index ranges	$-13 \le h \le 12$	$-13 \le h \le 12$	
	$0 \le k \le 19$	$0 \le k \le 19$	
	$0 \le l \le 9$	$0 \le l \le 9$	
D_{calc} (g/cm^3)	3.516	3.507	
Absorption coefficient; Mo*K*α (mm^{-1})	17.32	17.28	
F(000)	784.0	784.0	
Collected reflections	2637	2649	
Unique reflections	2347	2360	
Observed reflections [$F_o > 4\sigma(F_o)$]	1136	775	
Final *R* [$F_o > 4\sigma(F_o)$]	0.090	0.151	
Largest diffraction peak and hole (e/Å^3)	1.82, –1.34	2.58, –2.01	

Results and discussion

Table 1 reports the unit-cell dimensions determined by least-squares refinement of the setting angles of 25 reflections. With increasing exposure time, the diffraction peaks became weaker and broader; crystallinity of the investigated realgar steadily worsened. The X-ray diffraction experiment was terminated after 30 h of light exposure because of loss of crystallinity. The *a* lattice parameter increased linearly and the *c* sinβ value increased because of the degradation of realgar exposed to light (Fig. 1). In contrast, the *b* lattice parameter remained substantially constant (Fig. 1). This characteristic is in complete agreement with the results of Bonazzi et al. (1996). Anisotropic variations of the lattice parameters led to a continuous increase of the unit-cell volume, which was

TABLE 2. Atomic coordinates and displacement parameters (Å²)

	x	*y*	*z*	U_{eq}	U_{11}	U_{22}	U_{33}	U_{23}	U_{13}	U_{12}
0h										
As1	0.1211 (2)	–0.0206 (1)	0.7635 (3)	0.0418 (5)	0.0426 (9)	0.0373 (9)	0.0456 (10)	–0.0034 (7)	0.0125 (7)	–0.0045 (6)
As2	0.4240 (2)	0.1388 (1)	0.8562 (3)	0.0406 (5)	0.0371 (8)	0.0378 (8)	0.0488 (10)	0.0005 (7)	0.0154 (6)	–0.0020 (6)
As3	0.3208 (2)	0.1264 (1)	1.1780 (3)	0.0405 (5)	0.0390 (8)	0.0429 (9)	0.0397 (9)	–0.0030 (7)	0.0111 (6)	–0.0005 (6)
As4	0.0395 (2)	0.1609 (1)	0.7147 (3)	0.0429 (5)	0.0370 (8)	0.0427 (9)	0.0481 (10)	0.0020 (7)	0.0106 (6)	0.0047 (6)
S1	0.3440 (4)	–0.0064 (3)	0.7007 (7)	0.0426 (8)	0.0454 (20)	0.0383 (18)	0.0475 (22)	–0.0024 (16)	0.0190 (17)	0.0054 (15)
S2	0.2138 (5)	–0.0234 (3)	1.1147 (7)	0.0426 (9)	0.0441 (20)	0.0393 (19)	0.0463 (22)	0.0042 (16)	0.0157 (17)	–0.0018 (15)
S3	0.2380 (5)	0.2261 (3)	0.6393 (7)	0.0440 (9)	0.0494 (21)	0.0381 (18)	0.0467 (22)	0.0080 (16)	0.0172 (17)	0.0032 (16)
S4	0.1071 (5)	0.2103 (3)	1.0522 (7)	0.0445 (9)	0.0441 (20)	0.0476 (21)	0.0456 (22)	–0.0017 (17)	0.0189 (17)	0.0073 (17)
6h										
As1	0.1229 (4)	–0.0209 (3)	0.7640 (7)	0.0456 (10)	0.0473 (18)	0.0386 (17)	0.0483 (22)	–0.0051 (15)	0.0089 (15)	–0.0050 (14)
As2	0.4234 (4)	0.1392 (3)	0.8548 (7)	0.0451 (10)	0.0423 (17)	0.0383 (17)	0.0567 (24)	0.0027 (16)	0.0172 (15)	–0.0034 (13)
As3	0.3206 (4)	0.1268 (3)	1.1761 (6)	0.0452 (10)	0.0469 (18)	0.0457 (18)	0.0425 (20)	–0.0043 (16)	0.0115 (15)	–0.0019 (15)
As4	0.0406 (4)	0.1607 (3)	0.7153 (7)	0.0479 (10)	0.0453 (18)	0.0458 (19)	0.0502 (23)	0.0028 (17)	0.0092 (15)	0.0047 (15)
S1	0.3461 (10)	–0.0062 (7)	0.7033 (17)	0.0475 (20)	0.0533 (45)	0.0418 (40)	0.0508 (52)	0.0066 (39)	0.0200 (39)	0.0047 (36)
S2	0.2138 (10)	–0.0225 (6)	1.1146 (16)	0.0458 (20)	0.0479 (41)	0.0386 (40)	0.0469 (51)	0.0049 (36)	0.0066 (36)	–0.0021 (33)
S3	0.2397 (11)	0.2246 (7)	0.6399 (18)	0.0507 (22)	0.0585 (50)	0.0396 (40)	0.0563 (58)	0.0101 (40)	0.0196 (43)	0.0053 (37)
S4	0.1068 (10)	0.2098 (7)	1.0494 (17)	0.0494 (21)	0.0502 (45)	0.0455 (43)	0.0540 (55)	–0.0049 (41)	0.0173 (39)	0.0110 (37)
12h										
As1	0.1241 (5)	–0.0206 (3)	0.7649 (8)	0.0598 (12)	0.0627 (24)	0.0500 (22)	0.0652 (28)	–0.0033 (20)	0.0149 (20)	–0.0071 (19)
As2	0.4235 (5)	0.1386 (3)	0.8541 (8)	0.0565 (12)	0.0500 (21)	0.0463 (20)	0.0753 (29)	0.0032 (19)	0.0206 (19)	0.0020 (16)
As3	0.3206 (5)	0.1266 (3)	1.1760 (7)	0.0554 (11)	0.0548 (22)	0.0558 (22)	0.0551 (24)	–0.0069 (19)	0.0142 (17)	–0.0047 (18)
As4	0.0415 (5)	0.1599 (3)	0.7152 (8)	0.0595 (12)	0.0553 (22)	0.0552 (23)	0.0635 (27)	0.0039 (20)	0.0082 (19)	0.0035 (19)
S1	0.3465 (12)	–0.0057 (8)	0.7041 (19)	0.0588 (25)	0.0597 (55)	0.0499 (50)	0.0710 (67)	0.0034 (48)	0.0251 (49)	0.0042 (43)
S2	0.2129 (12)	–0.0219 (8)	1.1141 (18)	0.0568 (23)	0.0591 (53)	0.0535 (52)	0.0611 (60)	0.0057 (46)	0.0222 (45)	0.0030 (44)
S3	0.2394 (14)	0.2256 (8)	0.6438 (20)	0.0650 (28)	0.0790 (71)	0.0442 (49)	0.0683 (69)	0.0107 (47)	0.0139 (55)	0.0061 (48)
S4	0.1065 (13)	0.2105 (9)	1.0466 (21)	0.0656 (28)	0.0632 (62)	0.0575 (57)	0.0773 (75)	–0.0044 (55)	0.0213 (54)	0.0087 (48)
18h										
As1	0.1254 (6)	–0.0205 (4)	0.7660 (9)	0.0653 (15)	0.0711 (30)	0.0530 (25)	0.0725 (33)	–0.0055 (23)	0.0206 (25)	–0.0081 (22)
As2	0.4229 (5)	0.1392 (4)	0.8517 (9)	0.0628 (14)	0.0557 (25)	0.0567 (26)	0.0812 (35)	0.0024 (24)	0.0272 (23)	0.0017 (21)
As3	0.3197 (6)	0.1267 (4)	1.1735 (9)	0.0646 (14)	0.0590 (27)	0.0647 (29)	0.0721 (32)	–0.0012 (25)	0.0212 (23)	–0.0019 (22)
As4	0.0412 (6)	0.1597 (4)	0.7151 (9)	0.0687 (15)	0.0580 (27)	0.0660 (30)	0.0802 (36)	0.0034 (27)	0.0154 (24)	0.0026 (23)
S1	0.3459 (14)	–0.0058 (9)	0.6994 (23)	0.0680 (32)	0.0662 (70)	0.0603 (67)	0.0833 (88)	0.0019 (62)	0.0298 (64)	0.0113 (55)
S2	0.2126 (13)	–0.0221 (10)	1.1123 (24)	0.0692 (33)	0.0546 (60)	0.0627 (67)	0.0948 (96)	–0.0007 (68)	0.0278 (61)	0.0002 (54)
S3	0.2388 (15)	0.2248 (10)	0.6421 (25)	0.0777 (39)	0.0704 (77)	0.0670 (77)	0.0927 (99)	0.0251 (73)	0.0165 (69)	0.0090 (62)
S4	0.1079 (16)	0.2110 (10)	1.0484 (28)	0.0818 (42)	0.0747 (82)	0.0627 (73)	0.1132 (118)	–0.0206 (77)	0.0344 (79)	0.0174 (63)
24h										
As1	0.1252 (15)	–0.0207 (10)	0.7617 (20)	0.0760 (37)	0.0884 (79)	0.0645 (71)	0.0732 (73)	–0.0036 (56)	0.0180 (60)	0.0010 (57)
As2	0.4248 (13)	0.1390 (8)	0.8502 (19)	0.0673 (33)	0.0785 (69)	0.0532 (59)	0.0750 (71)	0.0032 (48)	0.0288 (55)	0.0050 (48)
As3	0.3211 (11)	0.1275 (8)	1.1714 (16)	0.0608 (30)	0.0629 (54)	0.0648 (64)	0.0544 (54)	–0.0075 (44)	0.0149 (42)	0.0045 (44)
As4	0.0379 (14)	0.1594 (11)	0.7147 (23)	0.0795 (39)	0.0749 (72)	0.0841 (88)	0.0825 (81)	0.0031 (66)	0.0260 (61)	0.0075 (61)
S1	0.3465 (32)	–0.0072 (18)	0.7044 (45)	0.0680 (70)	0.0880 (166)	0.0408 (112)	0.0788 (154)	0.0023 (103)	0.0282 (130)	–0.0368 (114)
S2	0.2131 (48)	–0.0246 (23)	1.1126 (51)	0.0872 (106)	0.1401 (299)	0.0550 (155)	0.0717 (171)	0.0124 (132)	0.0371 (187)	0.0434 (181)
S3	0.2416 (35)	0.2263 (21)	0.6439 (48)	0.0706 (69)	0.0865 (176)	0.0541 (140)	0.0700 (156)	–0.0083 (118)	0.0189 (135)	–0.0048 (123)
S4	0.1081 (39)	0.2121 (26)	1.0342 (50)	0.0793 (78)	0.0942 (198)	0.0764 (187)	0.0685 (162)	0.0027 (143)	0.0236 (146)	–0.0018 (156)

799.5(3) Å³ before light treatment and reached 810.4(8) Å³ after 24 h of exposure.

Geometrical variations in the As_4S_4 molecule induced by light serve as a key to resolving degradation dynamics in realgar. We considered the relationship between the increasing unit-cell volume and the arrangement of As_4S_4 cage molecules in the lattice, or how the lattice expands anisotropically. Results of the crystal structure analyses are listed in Table 2. The crystal structure of realgar for each light exposure comprises covalently bonded As_4S_4 cages up to 24 h, which are generally identical to those previously reported (α-As_4S_4) (Ito et al. 1952; Pen'kov and Safin 1972; Forneris 1969; Mullen and Nowacki 1972; Bues et al. 1983; Bryndzia and Kleppa 1988). Figure 2 shows variations of bond distances in the As_4S_4 molecule as a function of exposure time. Bonazzi et al. (1996) surmised that the As_4S_4 molecules in realgar are altered into an expanded, less-ordered β phase (called χ phase) with light-induced degradation: the unit-cell expansion was ascribed mainly to As_4S_4 molecule expansion. However, there is no close correlation in the present study between the continuous increase of unit-cell volume and bond-distance variations in As_4S_4 molecules (Fig. 2). The volumes of the As_4S_4 cage were calculated using the IVTON program (Balić-Žunić and Vickovic 1996) to verify that the As_4S_4 molecule hardly expands at all during light exposure. The calculated geometrical parameters (volume, sphericity, and centroid of the cage) are listed in Table 5 and shown in Figure 3. The parameters show that the volume of the cage remains fairly constant during light exposure (Fig. 3). Volumes in the other cages of arsenic sulfide have been calculated as 14.755 Å³ for the As_4S_4 cage in synthetic β-As_4S_4 (Porter and Sheldrick 1972), 15.822 Å³ for the As_4S_4 cage in synthetic As_4S_4(II) (Kutoglu 1976), 15.650 Å³ for the As_4S_4 cage in pararealgar (Bonazzi et al. 1995), and 21.101 Å³ for the As_4S_5 cage in uzonite (Bindi et al. 2003). Consequently, the volumes of the As_4S_4 cages in realgar from this experiment (Table 5) are almost identical to that of β-As_4S_4. Moreover, the volumes are radically distinct from that of pararealgar.

Sphericity parameters can be used as a measure of the degree of deformation and polyhedral-shape irregularity (Berlepsch et al. 1999). The remaining sphericity parameter in the present study

TABLE 3. Intramolecular bond distances (Å) and angles (°) for realgar

Exposure time (h)		0	6	12	18	24
As1	-S2	2.230(5)	2.226(10)	2.225(12)	2.209(16)	2.215(29)
	-S1	2.240(4)	2.239(9)	2.232(11)	2.235(13)	2.244(36)
	-As4	2.570(2)	2.572(5)	2.562(6)	2.564(7)	2.570(20)
S2	-As1-S1	94.9(1)	94.5(3)	94.7(4)	95.6(5)	94.2(1.4)
	-As1-As4	99.2(1)	98.8(2)	98.9(3)	99.2(4)	99.5(8)
S1	-As1-As4	98.7(1)	98.8(2)	98.9(3)	99.1(3)	100.6(8)
As2	-S3	2.247(4)	2.222(10)	2.225(11)	2.227(14)	2.230(33)
	-S1	2.248(4)	2.236(10)	2.234(12)	2.239(14)	2.242(25)
	-As3	2.571(2)	2.559(6)	2.562(7)	2.562(7)	2.561(15)
S3	-As2-S1	94.3(1)	94.5(3)	95.0(4)	94.4(5)	95.5(1.1)
	-As2-As3	99.1(1)	99.2(3)	99.4(3)	98.4(4)	97.9(9)
S1	-As2-As3	99.5(1)	99.3(3)	98.5(3)	99.5(4)	98.5(8)
As3	-S4	2.240(4)	2.243(9)	2.241(11)	2.244(14)	2.275(36)
	-S2	2.249(4)	2.243(9)	2.261(12)	2.249(14)	2.286(41)
	-As2	2.571(2)	2.559(6)	2.562(6)	2.562(7)	2.561(15)
S4	-As3-S2	95.1(1)	94.6(3)	94.3(4)	94.8(5)	94.9(1.3)
	-As3-As2	99.4(1)	99.2(3)	98.6(3)	98.9(5)	97.3(9)
S2	-As3-As2	99.0(1)	99.2(3)	99.1(3)	99.3(4)	99.4(9)
As4	-S3	2.232(4)	2.215(11)	2.212(14)	2.219(15)	2.158(36)
	-S4	2.235(5)	2.229(10)	2.219(13)	2.229(17)	2.274(33)
	-As1	2.570(2)	2.572(5)	2.562(6)	2.564(7)	2.570(20)
S3	-As4-S4	94.9(1)	94.8(4)	93.6(4)	93.4(6)	90.7(1.3)
	-As4-As1	99.9(1)	99.3(2)	99.9(3)	99.3(4)	98.4(9)
S4	-As4-As1	99.9(1)	100.0(2)	100.3(3)	100.0(4)	101.1(1.1)

TABLE 4. Binding energies (eV) of individual photoemission features

Exposure time (h)	0	6	12	18	24	30
As3*d*	43.8	43.8	43.7	43.5	43.6	43.2
As3$p_{3/2}$	143.0	142.9	143.1	142.9	142.7	142.5
As3$p_{1/2}$	148.0	147.9	147.9	147.8	147.6	147.2
S2*p*	164.0	163.6	163.6	163.4	163.0	162.8
S2*s*	227.3	227.9	227.7	227.7	227.7	227.6
O1*s*	532.6	533.1	533.1	532.7	532.4	531.9

TABLE 5. As_4S_4 geometrical parameters calculated with the IVTON program (Balić-Žunić and Vickovic 1996)

Exposure time (h)	0	6	12	18	24
Volume (Å^3)	14.856	14.686	14.674	14.708	14.860
Average distance to ligands (Å)	2.143	2.135	2.134	2.135	2.140
Sphericity	0.906	0.908	0.909	0.908	0.912
Centroid-Centroid distance (Å)	5.642	5.643	5.648	5.659	5.665

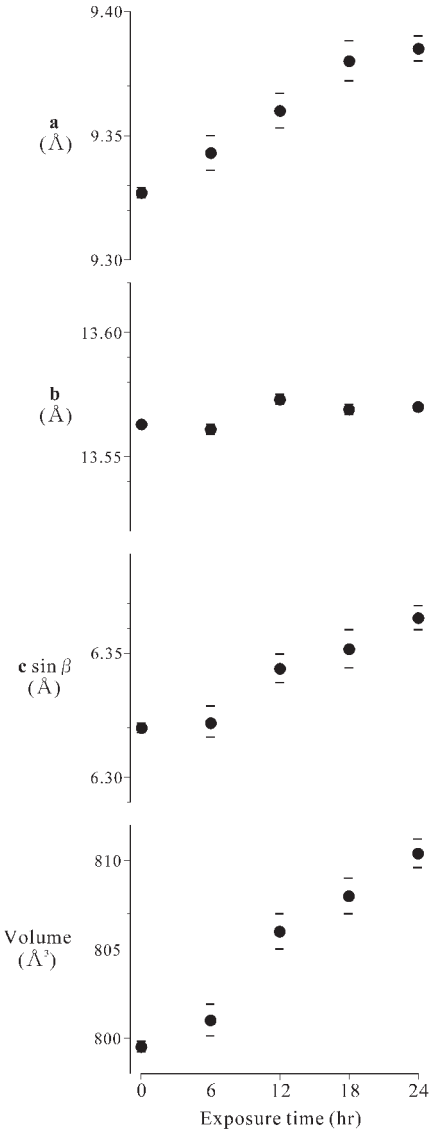

FIGURE 1. The *a*, *b*, *c*, and sinβ parameters and unit-cell volume vs. exposure time.

(Fig. 3) means that the light-induced degradation causes no distortion and irregularity of the As_4S_4 molecule. Therefore, the unit-cell expansion with light exposure is not entirely associated with both expansion and geometrical alteration in the As_4S_4 molecule. However, the most pronounced change during light exposure was the distance between centroids in the As_4S_4 cages, which continuously increased from 5.642 to 5.665 Å (Fig. 3 and Table 5). This observation implies that the spread of As_4S_4 intermolecular distance contributes to the unit-cell volume expansion.

High-resolution photoemission data for samples irradiated in air were acquired for the As 3*d*, As 3*p*, S 2*p*, S 2*s*, and O1*s* features (Fig. 4). Bullen et al. (2003) noted that the core-level spectra of realgar and pararealgar can be distinguished by small differences (0.1 eV) in core-level binding energies: the As3$d_{5/2}$ and S2$p_{3/2}$ peaks are at 43.1 and 162.8 eV, respectively, in realgar and 43.2 and 162.7 eV, respectively, in pararealgar. The variations of binding energies in the present study (Table 4) are remarkably larger than the difference between those of realgar and pararealgar reported by Bullen et al. (2003). Comparison with peak profiles during light exposure shows no obvious changes in the As3*p*, As3*d*, and S2*s* spectra (Fig. 4). Notwithstanding, the shoulder in the S2*p* spectra becomes markedly smaller as exposure time increases (Fig. 4b). The shoulder is inferred to result from disturbance of S atoms in altered realgar. Furthermore, the intensity of the O1*s* spectrum increases rapidly with exposure to light (Fig. 4d). The O1*s* spectrum is broad and consists of contributions from chemisorbed oxygen (lower BE) and arsenic oxides (higher BE) (Ghita et al. 2003). Ghita et al. (2003) stated that the As3*d* spectrum attributed to the arsenic oxide species As_2O_3 and As_2O_5 is located at about 44.0 and 45.3 eV, respectively. As seen in Figure 4a, the As3*d* spectrum

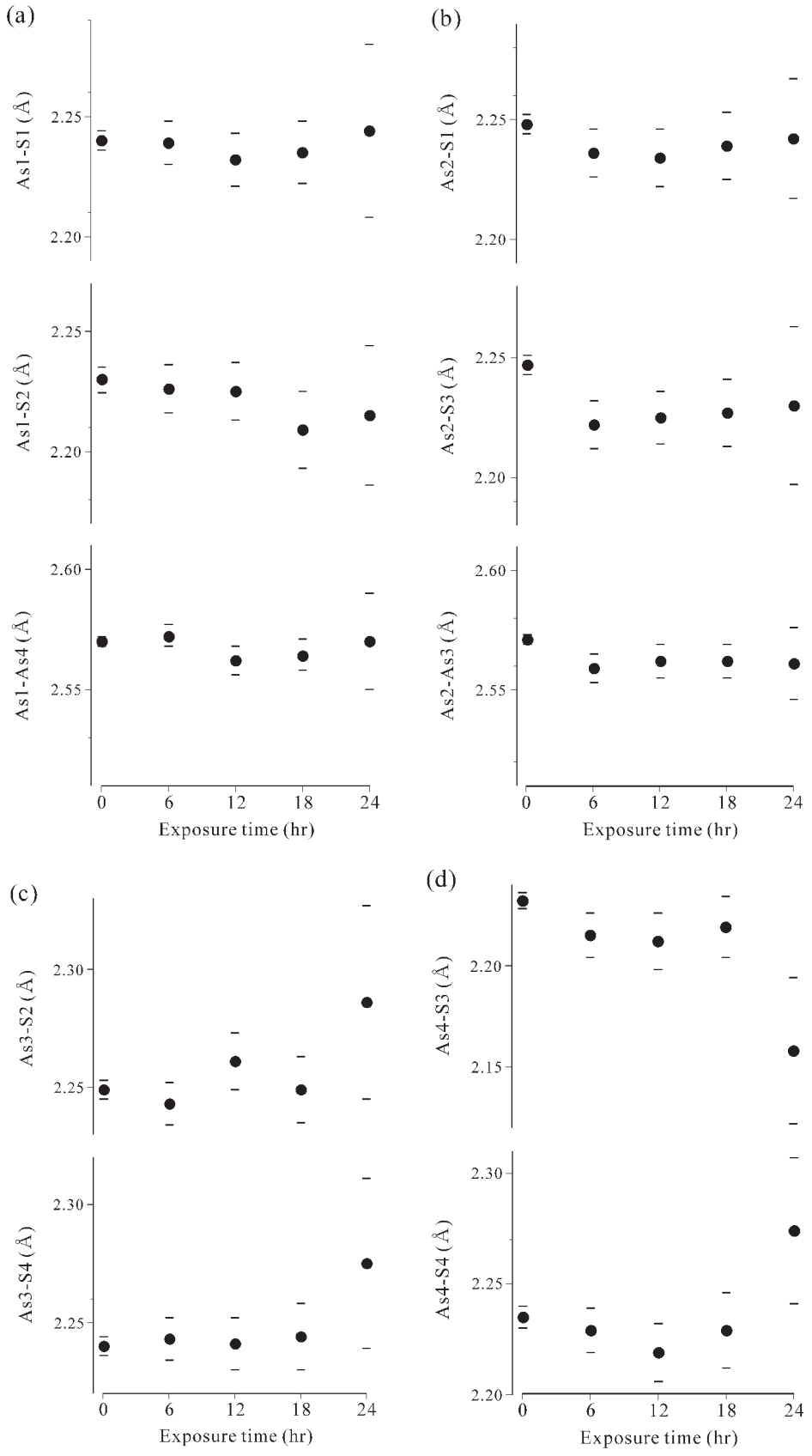

FIGURE 2. Plots showing changes in (**a**) As1 bond distances, (**b**) As2 bond distances, (**c**) As3 bond distances, and (**d**) As4 bond distances during light exposure.

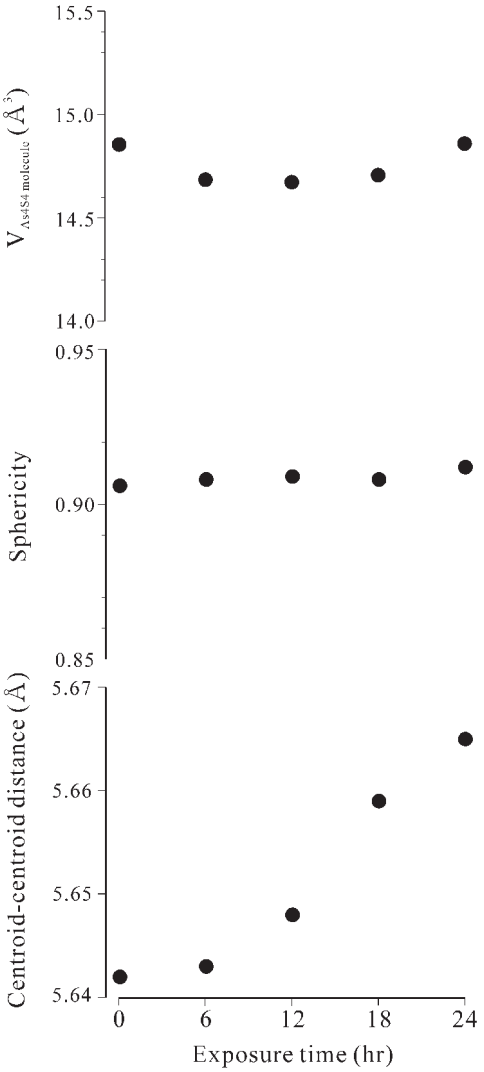

FIGURE 3. Variations of polyhedral parameters and distances between centroids in As_4S_4 cages as a function of exposure time.

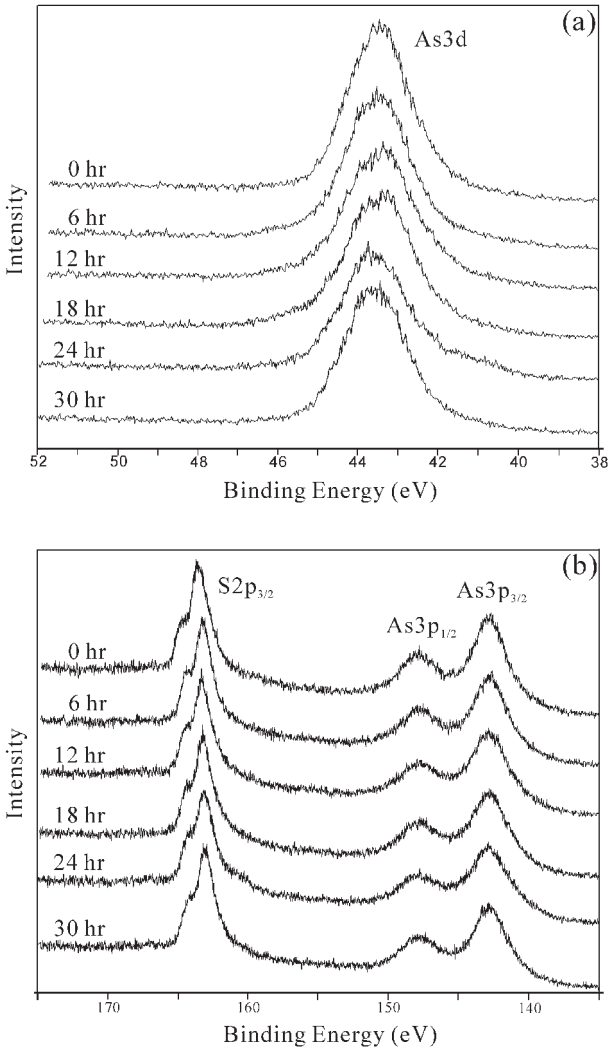

FIGURE 4. High-resolution core level XPS spectra of (**a**) As3*d*, (**b**) As3*p* and S2*p*, (**c**) S2*s*, and (**d**) O1*s* with increasing exposure times. *(Parts c and d on next page.)*

corresponding to arsenic oxide species can be identified as As_2O_3 rather than As_2O_5. The occurrence of arsenolite As_2O_3 as a product of the alteration of realgar was reported by Ballirano and Maras (2002). Bindi et al. (2003) showed that the expansion of unit-cell volume induced by lighting is attributable to an increase of As_4S_5 molecules in the structure, which results from the following reaction: $5As_4S_4 + 3O_2 \rightarrow 4As_4S_5 + 2As_2O_3$. The appearance of the O1*s* peak due to chemisorbed oxygen and arsenolite As_2O_3 in the present study has substantiated the formation of As_4S_5 molecule with light exposure. Moreover, it is noteworthy that the intensity of O1*s* peak appears not to increase continuously with increasing exposure time.

To clarify whether or not oxygen content is associated with the transformation, the light alteration experiment was performed in ultrahigh vacuum condition. Consequently, realgar was transformed into pararealgar as well, although small concentrations of oxygen were present on the surface before the transformation. It should be noted that the intensity of the O1*s* peak remained unchanged during the light alteration experiment under ultrahigh vacuum conditions. The results strongly suggests that the transformation proceeds by light if there is a small amount of oxygen. That is, the reaction $5As_4S_4 + 3O_2 \rightarrow 4As_4S_5 + 2As_2O_3$ need not occur throughout the light exposure. This evidence is substantiated by XPS measurements in air: the intensity of the O1*s* spectrum remains fairly constant after increasing the peak by light exposure (Fig. 4d). Therefore, it seems reasonable to consider the following process: the As_4S_5 molecule is created temporarily by the reaction $5As_4S_4 + 3O_2 \rightarrow 4As_4S_5 + 2As_2O_3$. Bindi et al. (2003) documented that the expansion of unit-cell volume induced by lighting is attributable to an increase of As_4S_5 molecules in the structure, which results from the following reaction: $5As_4S_4 + 3O_2 \rightarrow 4As_4S_5 + 2As_2O_3$. The formation of As_4S_5 molecules in the structure is convenient to cause both anisotropic expansion of the unit-cell volume and the phase transformation from realgar to pararealgar. First, adding

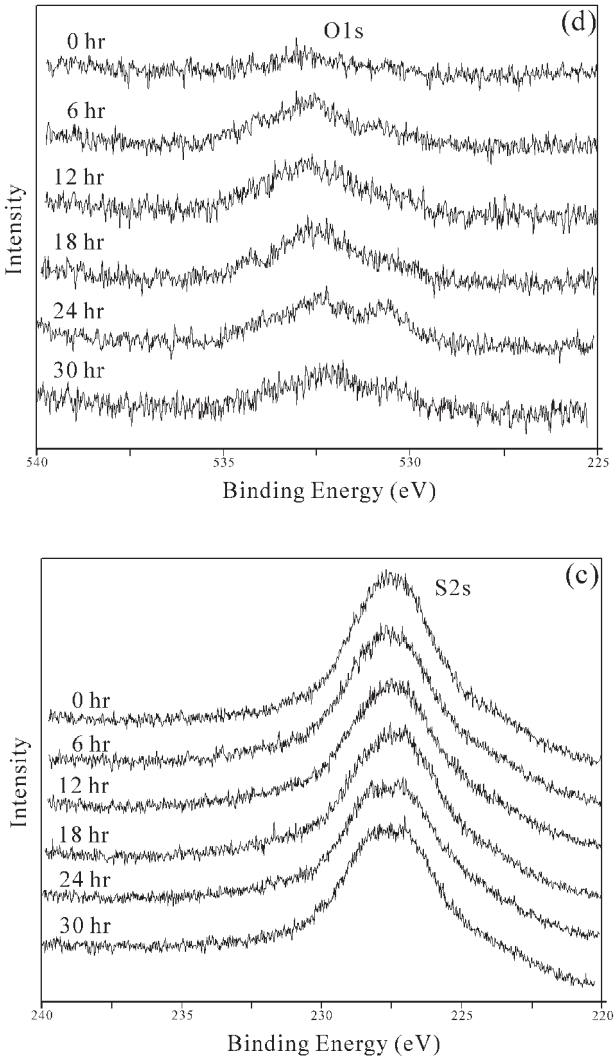

FIGURE 4. *Parts c and d. Continued from previous page.)*

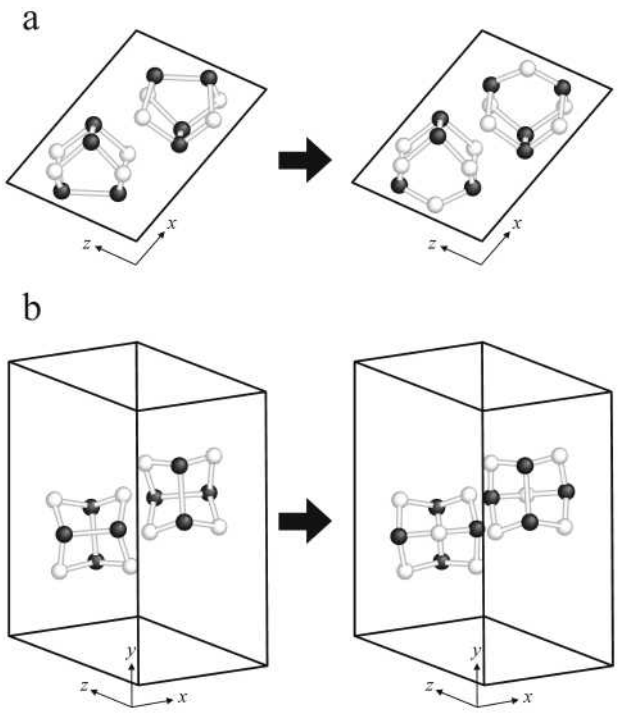

FIGURE 5. The crystal structures of realgar in projections along (**a**) [010] and (**b**) [4$\bar{1}$4]. As atoms and S atoms are shown as black and white spheres.

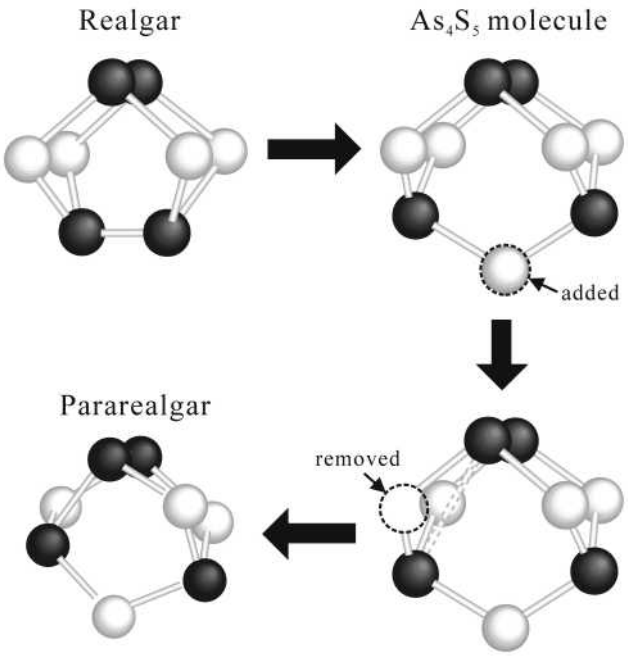

FIGURE 6. Molecular structures of realgar, As_4S_5, and pararealgar. The arrow shows the processes of phase transformation from realgar to pararealgar. As atoms and S atoms are shown as black and white spheres.

an S atom into the As_4S_4 molecule can compel unit-cell expansion in the **a** and **c** directions rather than the **b** direction (Fig. 5). The additional S atom is inserted between the As atoms in the As_4S_4 molecule because As-As bonds are weaker than As-S bonds (Douglass et al. 1992). Thereby, the direction for the additional S atoms points toward [4$\bar{1}$4] in the unit cell of realgar (Fig. 5); it becomes a main factor governing the elongation of **a** and **c** rather than **b**. This may be the reason why the standard deviation of *b* is constant whereas that of *a*, *c*, and β grow with exposure time. Secondly, the As_4S_4 molecular structure of realgar can transform more easily into that of pararealgar via the As_4S_5 molecule than directly into pararealgar (Fig. 6). We infer this process: the As_4S_4 molecule in realgar transforms into the As_4S_5 molecule with incorporation of an S atom (Fig. 6). However, the additional S atom would lead to varied point charges on the other atoms in the molecule. It is likely that the resulting As_4S_5 molecule is too unstable to exist under the collapsed electrostatic potentials. Consequently, an S atom is released from an equivalent As-S-As linkage in the As_4S_5 molecule, which turns into the As_4S_4 molecule of the pararealgar type (Fig. 6). After the As_4S_5 molecule is divided into an S atom (radical) and an As_4S_4 (pararealgar type) molecule, the free S

atom is re-attached to another As_4S_4 (realgar type) molecule, and reproduces an As_4S_5 molecule. The reproduced As_4S_5 molecule is again divided into an S atom (radical) and an As_4S_4 (pararealgar type) molecule. This cycle is promoted by light and repeated during light exposure. Moreover, the cycle makes it possible for realgar to transform into pararealgar under the low concentrations of oxygen. Finally, on the basis of the above observation and consideration, we speculate that the As_4S_4 molecular in pararealgar and the residual As_4S_5 molecules (lower crystallinity) might ultimately co-exist in altered materials because arsenic sulfide minerals with chemical compositions ranging continuously from As_8S_8 to As_8S_9 can crystallize (Bonazzi et al. 2003).

ACKNOWLEDGMENTS

The single-crystal X-ray data collections were carried out at the Research Facility Center for Science and Technology, University of Tsukuba. This work was partially supported by a research grant to A.K. from the Saneyoshi Scholarship Foundation. The paper benefited from perceptive reviews by two anonymous reviewers and editorial attention by S. Quartieri.

REFERENCES CITED

Balić-Žunić, T. and Vickovic, I. (1996) IVTON—program for the calculation of geometrical aspects of crystal structures and some crystal chemical applications. Journal of Applied Crystallography, 29, 305–306.

Ballirano, P. and Maras, A. (2002) Preliminary results on the light-induced alteration of realgar: kinetics of the process. Plinius, 28, 35–36.

——— (2004) The light-induced alteration of realgar (As_4S_4): an in-situ X-ray powder diffraction investigation. I-kinetics of the process. 32nd International Geological Congress Program and Abstract, 489.

Berlepsch, P., Miletich, R., and Armbruster, T. (1999) The crystal structures of synthetic KSb_5S_8 and $(Tl_{0.598},K_{0.402})Sb_5S_8$ and their relation to parapierrotite ($TlSb_5S_8$). Zeitschrift für Kristallographie, 214, 57–63.

Bindi, L., Popova, V., and Bonazzi, P. (2003) Uzonite, As_4S_5, from the type locality: single-crystal X-ray study and effects of exposure to light. Canadian Mineralogist, 41, 1463–1468.

Bonazzi, P., Menchetti, S., and Pratesi, G. (1995) The crystal structure of pararealgar, As_4S_4. American Mineralogist, 80, 400–403.

Bonazzi, P., Menchetti, S., Pratesi, G., Muniz-Miranda, M., and Sbrana, G. (1996) Light-induced variations in realgar and β-As_4S_4: X-ray diffraction and Raman studies. American Mineralogist, 81, 874–880.

Bonazzi, P., Bindi, L., Olmi, F., and Menchetti, S. (2003) How many alacranites do exist? A structural study of non-stoichiometric As_8S_{9-x} crystals. European Journal of Mineralogy, 15, 283–288.

Bryndzia, L.T. and Kleppa, O.J. (1988) Standard molar enthalpies of formation of realgar (α-AsS) and orpiment (As2S3) by high-temperature direct-synthesis calorimetry. Journal of Chemical Thermodynamics, 20, 755–764.

Bues, W., Somer, M., and Brockner, W. (1983) Schwingungsspektren von As_4S_4 und As_4Se_4. Zeitschrift für anorganische und allgemeine Chemie, 499, 7–14.

Bullen, H.A., Dorko, M.J., Oman, J.K., and Garrett, S.J. (2003) Valence and core-level binding energy shifts in realgar (As_4S_4) and pararealgar (As_4S_4) arsenic sulfides. Surface Science, 531, 319–328.

Burns, P.C. and Percival, J.B. (2001) Alacranite, As_4S_4: a new occurrence, new formula, and determination of the crystal structure. Canadian Mineralogist, 39, 809–818.

Clark, A.H. (1970) Alpha-arsenic sulfide, from Mina Alacrán, Pampa Larga, Chili. American Mineralogist, 55, 1338–1344.

Douglass, D.L., Shing, C., and Wang, G. (1992) The light-induced alteration of realgar to pararealgar. American Mineralogist, 77, 1266–1274.

Enraf, N. (1983) Structure determination package (SDP). Enraf Nonius, Delft, The Netherlands.

Forneris, R. (1969) The infrared and Raman spectra of realgar and orpiment. American Mineralogist, 54, 1062–1074.

Ghita, R.V., Negrila, C., Manea, A.S., Logofatu, C., Cernea, M., and Lazarescu, M.F. (2003) X-ray photoelectron spectroscopy study on n-type GaAs. Journal of Optoelectronics and Advanced Materials, 5, 859–863.

Ito, T., Morimoto, N., and Sadanaga, R. (1952) The crystal structure of realgar. Acta Crystallographica, 5, 775–782.

Kutoglu, V.A. (1976) Darstellung und kristallstruktur einer neuen isomeren form von As_4S_4. Zeitschrift für anorganische und allgemeine Chemie, 419, 176–184.

Mullen, D.J.E. and Nowacki, W. (1972) Refinement of the crystal structures of realgar, AsS and orpiment, As_2S_3. Zeitschrift für Kristallographie, 136, 48–65.

Pen'kov, L.N. and Safin, L.A. (1972) Nuclear quadrupole resonance in realgar. Doklady Akademii Nauk SSSR Novaia Seriia, 153, 144–146.

Porter, E.J. and Sheldrick, G.M. (1972) Crystal structure of a new crystalline modification of tetra-arsenic tetrasulphide (2,4,6,8-tetrathia-1,3,5,7-tetra-arsatricyclo[3,3,0,0]-octane). Journal of the American Chemical Society Dalton, 13, 1347–1349.

Roberts, A.C., Ansell, H.G., and Bonardi, M. (1980) Pararealgar, a new polymorph of AsS, from British Columbia. Canadian Mineralogist, 18, 525–527.

Roland, G.W. (1972) Concerning the α-AsS realgar inversion. Canadian Mineralogist, 11, 520–525.

Sheldrick, G.M. (1997) SHELXL-97. A program for crystal structure refinement. University of Göttingen, Germany.

Street, B.G. and Munir, Z.A. (1970) The structure and thermal properties of synthetic realgar (As_4S_4). Journal of Inorganic Nuclear Chemistry, 32, 3769–3774.

Yu, S.C. and Zoltai, T. (1972) Crystallography of a high-temperature phase of realgar. American Mineralogist, 57, 1873–1876.

MANUSCRIPT RECEIVED AUGUST 12, 2005
MANUSCRIPT ACCEPTED FEBRUARY 11, 2005
MANUSCRIPT HANDLED BY SIMONA QUARTIERI